Persistent luminescence in powdered and ceramic polycrystalline $Gd_3Al_2Ga_3O_{12}$:Ce

To cite this article: G Dosovitskiy *et al* 2017 *IOP Conf. Ser.: Mater. Sci. Eng.* **169** 012014

Persistent luminescence in powdered and ceramic polycrystalline $Gd_3Al_2Ga_3O_{12}$:Ce

G Dosovitskiy[1], A Fedorov[2], V Mechinsky[3], A Borisevich[3], A Dosovitskiy[4], E Tret'jak[5], M Korjik[2,3]

[1] Institute of Chemical Reagents and High Purity Chemical Substances IREA, 107076 Moscow, Russia
[2] Radiation Instruments and New Components, 220113 Minsk, Belarus
[3] Research Institute for Nuclear Problems, 220030 Minsk, Belarus
[4] NeoChem, 117647 Moscow, Russia
[5] Research Institute for Physical Chemical Problems, 220030 Minsk, Belarus

E-mail: george.dos@gmail.com

Abstract. This paper studies powders of $Gd_3Ga_3Al_2O_{12}$:Ce, a promising scintillator composition, as a possible object for express pre-characterization of scintillation kinetics and level of persistent luminescence. Garnet phase powders with uniform microstructure, consisting of 1-2 μm grains, were obtained by co-precipitation approach. It was shown, that both scintillation decay time and presence of persistent luminescence are influenced by both powder thermal treatment temperature and strong Ga deficit.

1. Introduction

Scintillator crystals and phosphors based on Ce-activated mixed garnets $Gd_3(Ga,Al)_5O_{12}$ (GGAG) get increasing interest recent years [1], as they have promising applications on large markets, such as medical imaging. Light yield of 55000 Ph/MeV was obtained for $Gd_3Ga_3Al_2O_{12}$:Ce transparent ceramic [2] and single crystal scintillators [3]. At the same time, strong persistent luminescence was observed for $Gd_3(Ga,Al)_5O_{12}$:Ce ceramics and single crystals grown from raw materials of 99,995% or better purity [2,4]. Moreover, garnets with Al/Ga solid solution turned out to be promising materials for long glowing phosphors – strong persistent luminescence was observed in $Y_3(Ga,Al)_5O_{12}$:Ce,Cr ceramic samples [5]. High level of afterglow is a major drawback in application of this material in scintillation detectors, so studying this effect and its minimizing is a mandatory and an important issue for its future application.

A number of works was dedicated to optimizing host compound composition. Ogiegło et al [6] found the most intensive photoluminescence in powder samples of $Gd_3Ga_xAl_{5-x}O_{12}$:Ce row at $x = 2$. For single crystalline materials the most used composition of choice is $Gd_3Ga_3Al_2O_{12}$:Ce [3,7-10].

As a complex oxide solid solution, GGAG system allows wide composition variations. Scintillation kinetics depending on composition was studied in a number of works [3,7-10], results are summarized in Table 1. One can see that kinetics data differ for identical compositions. Inhomogeneous element distribution could have effect on scintillation properties, such inhomogeneity was reported e.g. for complex $(Lu,Gd)_3(Ga,Al)_5O_{12}$:Ce garnet crystals grown by micropulling-down technique [7]. One of possible reasons for that is incontrollable Ga content in a crystal. According to thermodynamic data, maximum evaporation rate of Ga oxide could reach $5*10^{-5}$ – $5*10^{-3}$ mol*cm^{-2}*s^{-1} in a temperature range 1800-2000 °C in oxidizing conditions [11]. It is known, that Gd_2O_3-Ga_2O_3 system has a substantial homogeneity range around a garnet phase – 4% according to [12] and 2,5% according to [13]. Wide homogeneity region accommodating Ga deficit was found for Y_2O_3-Gd_2O_3-Ga_2O_3-Al_2O_3 system in [2]. Certain homogeneity region was found for Gd_2O_3-Ga_2O_3-Al_2O_3 system as well [14], which means that scintillator could accommodate a lot of defects, caused by Ga deficit, and still comprise a single-phase garnet.

Table 1. Scintillation kinetics of GGAG, depending on composition, basing on data from [3,7-10].

Reference:		Composition: $Gd_3Ga_xAl_{(5\text{-}x)}O_{12}$:Ce			
		x=3	x=2.7	x=2.4	x=2
[3]	LY, Ph/MeV	55 000	58 000	46 000	
	τ_{sc}, ns (P, %)	97 (80) 353 (20)	172 (88) 1932 (12)	138 (71) 649 (29)	
[7]	LY, Ph/MeV	42 217			45 931
	τ_{sc}, ns (P, %)	52.8 (73) 282 (27)			221 (100)
[8]	LY, Ph/MeV	56 500	55 600	44 600	
	τ_{sc}, ns (P, %)	150(61) 490 (39)	150(61) 490 (39)	130(42) 620(31) 6700(27)	
[9]	LY, Ph/MeV	45 260		40 740	
	τ_{sc}, ns (P, %)	89(73) 286(27)		136(69) 647(31)	
[10] (10x10x10 mm)	LY, Ph/MeV	35 600			
	τ_{sc}, ns (P, %)	156(76) 565(24)			
[10] (2x2x10 mm)	LY, Ph/MeV	34 700			
	τ_{sc}, ns (P, %)	101(65) 319(35)			

Influence of Ga deficit on persistent luminescence is controversial yet. As could be concluded from [2], Ga deficit could be a possible reason for persistent luminescence in $Gd_{1.49}Y_{1.49}Ce_{0.02}Ga_{2.2}Al_{2.8}O_{12}$ ceramics. In [1], on the contrary, composition shift towards excess of Gd leads to increase of light yield and decrease of afterglow in powders with compositions close to $(Gd_{0.988}Ce_{0.012})_3(Al_{0.56}Ga_{0.44})_5O_{12}$.

Existence of correlation between luminescent properties of GGAG polycrystalline ceramic samples and single crystals of corresponding composition was shown in [15], which justifies using polycrystalline samples for preliminary studies of single crystal scintillators.

In order to define an origin of persistent luminescence in $Gd_3Al_2Ga_3O_{12}$:Ce we have examined microstructure properties and scintillation kinetics of powder samples and ceramics, which are synthesized at temperatures up to 1600 °C. Ga volatility is much lower at these conditions, so powder composition could be better determined then for crystals.

2. Experimental

2.1. Samples preparation

Powders were obtained by co-precipitation technique. Nitrate solutions with 1 mole/l concentrations were prepared from Gd oxide (5N), Ga nitrate (4N), Al nitrate (5N), NH_4-Ce nitrate (4N), then mixed in proportion to match desired composition of $Gd_{2.97}Ce_{0.03}Ga_{3-x}Al_2O_{12}$. This joint solution was added to ammonia solution with concentration 2.5 mole/l at a rate 30 ml/min with constant stirring. Then the precipitate slurry was kept boiling for 30 minutes, then filtered, washed with water, dried at 100 °C, crushed, sieved through 100 μm sieve and calcined at 600 °C and then sintered at 1000-1600 °C in air for 2 hours in molten silica or corundum crucibles.

2.2. Samples characterization

Powders microstructure was observed using Jeol JSM 7100 F scanning electron microscope with EDX detector Oxford Instruments X-max^N for local element analysis. Powder X-ray diffractometer GBC Scientific eMMA with Cu K_α radiation was used for phase analysis. Thermogravimetry and differential thermal analysis were performed using Thermo Scientific SDT Q600 analyzer. Photoluminescence spectra were measured using Lumex Fluorat-02-Panorama spectrometer with a fiber lightguide attachment.

2.3. Scintillation measurements

^{22}Na source with gamma emission lines of 511 keV and 1,27 MeV and activity of 1000 Bq was used for scintillation measurements. Decay curves were registered in 1 μs range using start-stop method with ratio of starts to stops 0.02.

3. Results and discussion

3.1. Composition and microstructure

When precipitation was conducted according to the procedure, which works for YAG precipitation [16], using excess of precipitant 20-50%, then 3-7% of Ga remained in mother solution. This corresponds to Ga hydroxide solubility in ammonia water solutions [17]. Boiling precipitate slurry for 30 minutes allows to decrease Ga losses to no more than 0.5%. Filtered and dried precipitate forms dense xerogel translucent pieces, consisting of 10-20 nm particles (Figure 1) with homogeneous elements (Gd, Ga, Al) distribution according to EDX mapping (Figure 2).

Heating the precipitate up to 1200 °C leads to a mass loss of 28%, which corresponds to processes of release of physically and chemically linked water and precipitate decomposition with transformation of Gd, Ga, Al, Ce hydroxides to oxide form. Exothermal peak is found at 880 °C on DTA curve, which, most probably, corresponds to garnet phase formation (Figure 3). In correspondence with this, powders sintered at 1000-1600 °C contain garnet phase (most close to PDF 73-1371) with peaks seemingly narrowing with temperature increase up to sintering temperature of 1400 °C, which indicates increase of their crystallinity with thermal treatment temperature (Figure 4).

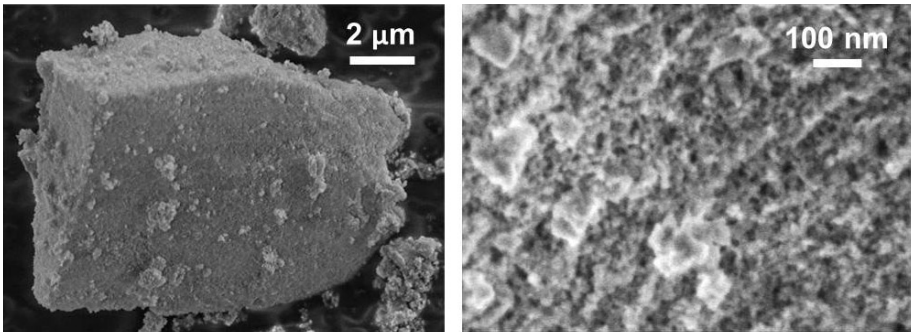

Figure 1. SEM images of a GGAG xerogel.

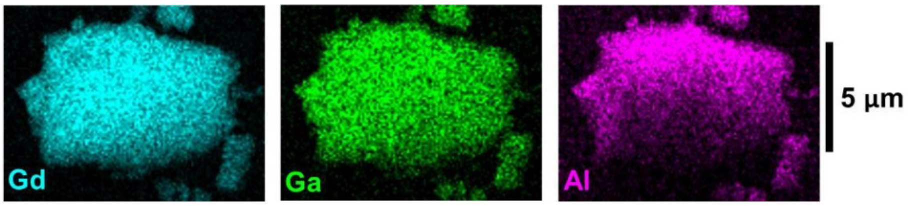

Figure 2. EDX element mapping of a GGAG xerogel particle.

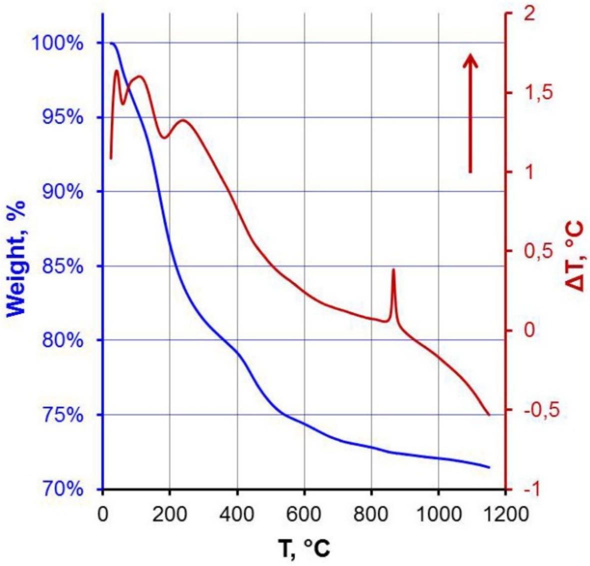

Figure 3. TG-DTA curve for GGAG precipitate, heating rate 10 °C/min.

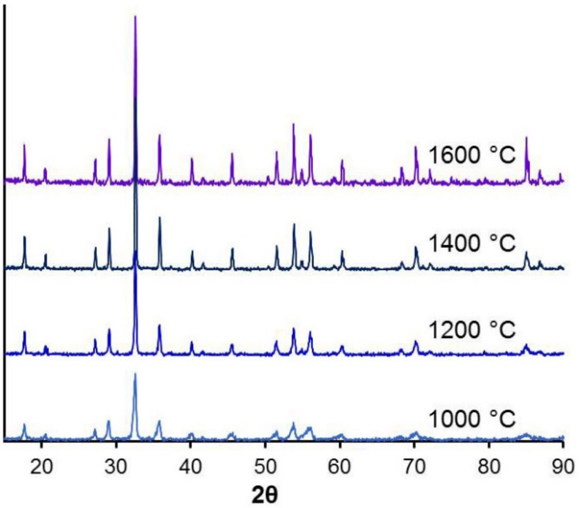

Figure 4. XRD patterns for GGAG powders, sintered at different temperatures

Samples microstructure observed by SEM gradually changes with powder sintering temperature increase (Figure 5). At lower sintering temperatures two types of grains could be seen on images: larger, 0.5-2 µm size and smaller, ~50 nm for 1000 °C and ~100 nm for 1200 °C. Powder particles contain noticeable amount of 50-100 nm pores. Raising sintering temperature leads to a more uniform microstructure: at 1400 °C 0.3-1 µm grains and 0.2-0.3 µm pores, at 1600 °C 1-2 µm grains and up to 1 µm pores (not shown on the image). Faceting of separate grains can be noticed after 1600 °C.

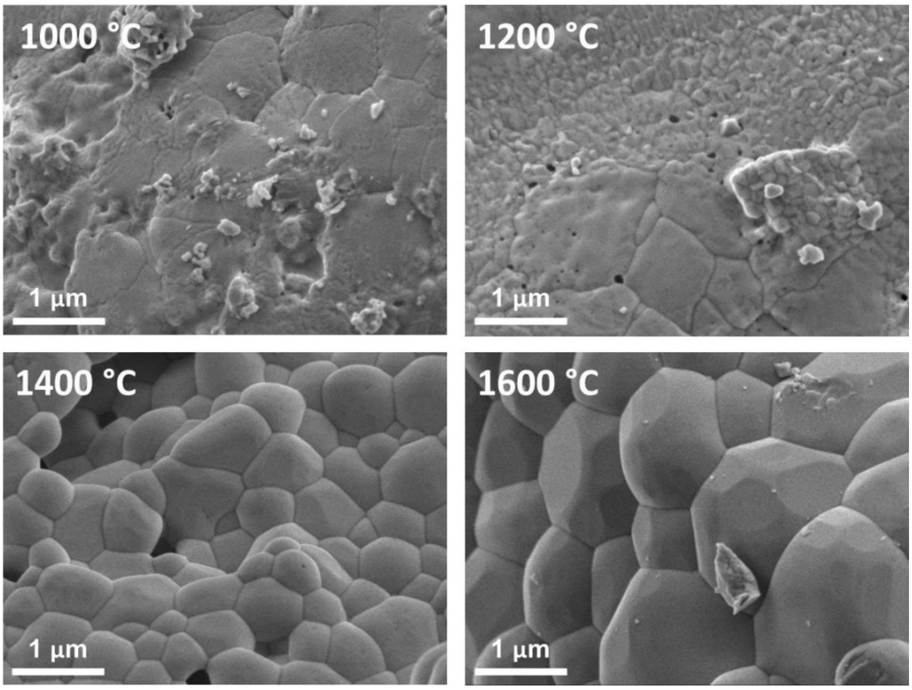

Figure 5. SEM images of a GGAG powder, sintered at different temperatures.

3.2. Luminescent and scintillation properties

Photoluminescence of obtained GGAG powders is typical for Ce-activated garnets with two broad excitation bands (4f-5d transitions $^2F_{5/2} \rightarrow {}^2D_{5/2}$ with maximum at 340 nm, $^2F_{5/2} \rightarrow {}^2D_{3/2}$ with maximum at 445 nm) and one emission band (5d-4f transition $^2D_{3/2} \rightarrow {}^2F_{7/2}$, $^2F_{5/2}$ with maximum at 535 nm) (Figure 6). Ga content variation ±1% does not change bands positions.

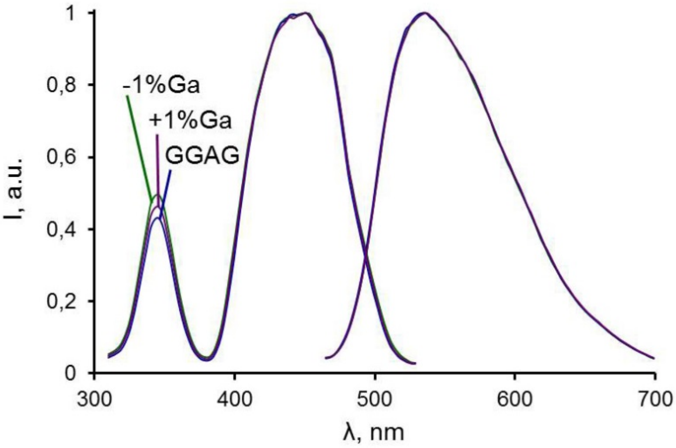

Figure 6. Photoexcitation and photoluminescence spectra (normalized) for GGAG powder with varying Ga content.

Scintillation decay curves were measured to determine samples scintillation kinetics. Background of random coincidences in scintillation kinetics measurements by start-stop method can be used for qualitative estimation of samples persistent luminescence. Light yields were not specially measured, as at the time of the research there was no appropriate technique to adequately estimate light yields on powder samples, to their values are not reported. They could be qualitatively estimated from necessary measurement time to collect enough statistics in kinetic measurements. According to that light yields were the same order of magnitude.

For all samples kinetics contained 2 or 3 exponential components, faster one (τ_1) around 40 ns? slower ones more than 100 ns and averaged scintillation time in the range of 54-81 ns (Table 2).

Comparing kinetics measurements for samples with different Ga content, one can state, that average scintillation time is higher for samples with 5% Ga deficit (70-80 ns) compared to samples with Ga variation of 1% (55-60 ns). Background level in kinetics measurements is close for them, tenting to be higher for Ga-deficit sample (Figure 7).

Effect of increase of sample thermal treatment temperature can be anticipated from comparison of measurements results for GGAG powder sintered at 1000 °C and GGAG ceramics of the same composition sintered at 1600 °C (Figure 8). It leads to insignificant change of scintillation decay curve and averaged scintillation decay time – 67 ns for 1000 °C powder and 72 ns for 1600 °C ceramics. At the same time, there is also a noticeable difference in background level, indicating that low temperature sample has noticeably lower level of persistent luminescence.

As a proposal for future work, described synthesis approach could be used to prepare homogeneous pre-synthesized raw materials for single crystal growth and test its influence on single crystalline material kinetics and level of persistent luminescence.

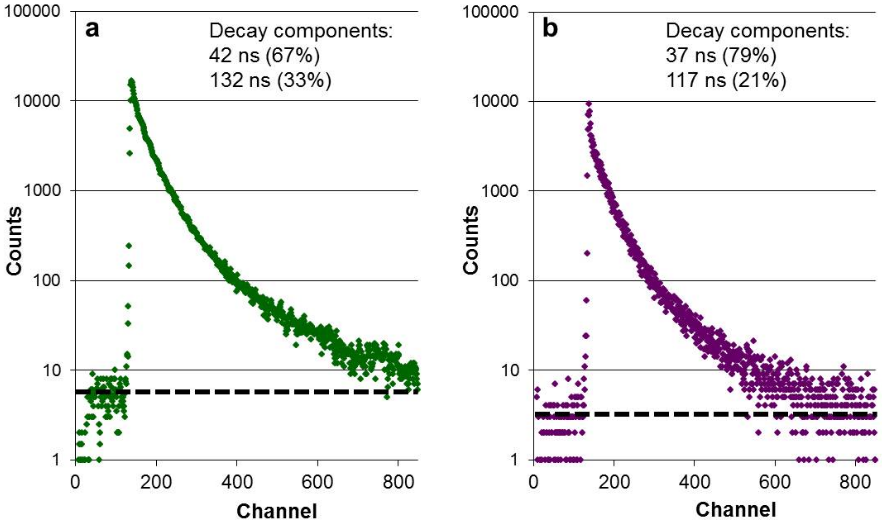

Figure 7. Scintillation decay curves for GGAG powder sintered at 1600 °C with composition $Gd_{2.97}Ce_{0.03}Ga_{2.85}Al_2O_{12}$ (a) and $Gd_{2.97}Ce_{0.03}Ga_3Al_2O_{12}$ (b). 1 channel equals 1 ns. Dashed line indicates background level estimation.

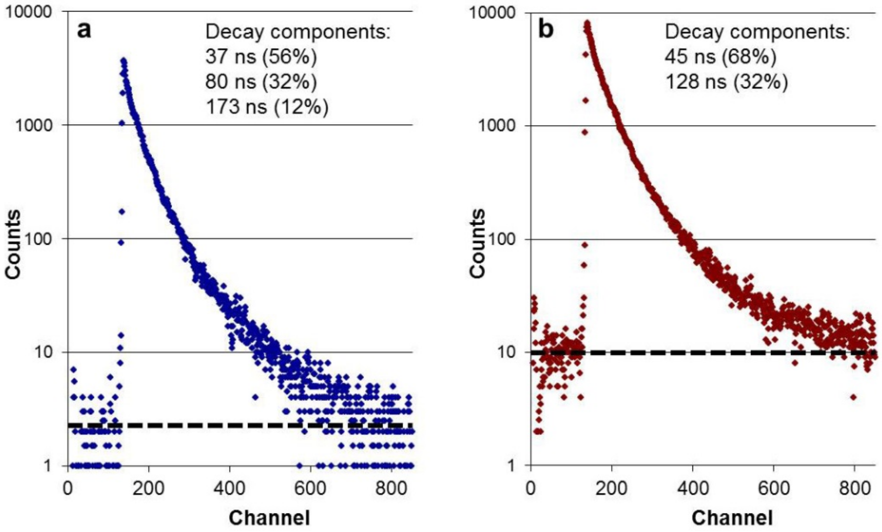

Figure 8. Scintillation decay curves for GGAG powder sintered at 1000 °C (a) and GGAG ceramics of the same composition sintered at 1600 °C (b). 1 channel equals 1 ns. Dashed line indicates background level estimation.

Table 2. Scintillation decay components for GGAG samples of different compositions: powder sintered at 1000 °C, ceramics sintered at 1600 °C, all other – powders sintered at 1600 °C.

Composition:	τ_1, ns	P_1, %	τ_2, ns	P_2, %	τ_3, ns	P_3, %	$\tau_{average}$, ns
$Gd_{2.97}Ce_{0.03}Ga_{\mathbf{3.03}}Al_2O_{12}$	48	81%	108	19%			60
$Gd_{2.97}Ce_{0.03}Ga_{\mathbf{3}}Al_2O_{12}$	37	79%	117	21%			54
$Gd_{2.97}Ce_{0.03}Ga_{\mathbf{2.97}}Al_2O_{12}$	41	59%	82	41%			58
$Gd_{2.97}Ce_{0.03}Ga_{\mathbf{2.85}}Al_2O_{12}$	42	67%	132	33%			70
$Gd_{2.97}Ce_{0.03}Ga_{\mathbf{2.85}}Al_2O_{12}$	47	72%	177	28%			81
$Gd_{2.97}Ce_{0.03}Ga_{\mathbf{2.85}}Al_2O_{12}$ 1000	37	56%	80	32%	172	12%	67
$Gd_{2.97}Ce_{0.03}Ga_{\mathbf{2.85}}Al_2O_{12}$ ceram.	45	67%	128	32%			72

4. Conclusions

Powder polycrystalline materials could be obtained with homogeneous composition, well-defined µm-size grains and well-formed garnet phase. Deficit of Ga in powder samples was shown to slow down scintillation kinetics, increasing averaged scintillation time from 55-60 ns to 70-80 ns. Slightly higher level of background in kinetic measurements was observed in these samples, indicating higher level of persistent luminescence. GGAG ceramics, heat treated at 1600 °C has shown higher level of afterglow, compared to powder heat treated at 1000 °C. So, to use polycrystalline samples as objects for express pre-characterization of single crystal materials, such temperature-dependent parameters as microstructure and crystallinity should be taken into account.

Acknowledgements

Work was supported by Russian Ministry of Science and Education, Subsidy agreement № 14.625.21.0033 dated 27.10.2015, project identifier RFMEFI62515X0033.

References

[1] Kanai T, Satoh M and Miura I 2008 *J. Am. Ceram. Soc.* **91** 456–62

[2] Seeley Z M, Cherepy N J and Payne S A 2013 *J. Cryst. Growth* **379** 79–83

[3] Kamada K *et al.* 2014 *Opt. Mater.* **36** 1942–5

[4] Wu Y, Luo Z, Jiang H, Meng F, Koschan M and Melcher C L 2015 *Nucl. Instr. Meth. A* **780** 45–50

[5] Ueda J, Kuroishi K and Tanabe S 2014 *Appl. Phys. Lett.* **104** 101904 1–4

[6] Ogiegło J M, Katelnikovas A, Zych A, Jüstel T, Meijerink A and Ronda C R 2013 *J. Phys. Chem. A* **117** 2479–84

[7] Kamada K, Endo T, Tsutumi K, Yanagida T, Fujimoto Y, Fukabori A, Yoshikawa A, Pejchal J and Nikl M 2011 Cryst. Growth Des. 11 4484–90

[8] Sibczynski P, Iwanowska-Hanke J, Moszyński M, Swiderski L, Szawłowsk M, Grodzicka M, Szczęśniak T, Kamada K and Yoshikawa A 2015 *Nucl. Instrum. Meth. A* **772** 112–7

[9] Sakthong O, Chewpraditkul W, Kamada K, Yoshikawa A, Szczesniak T, Grodzicka M, Sibczynski P, Moszynski M 2016 *Rad. Meas.* **87** 24–28

[10] Lucchini M T, Babin V, Bohacek P, Gundacker S, Kamada K, Nikl M, Petrosyan A, Yoshikawa A and Auffray E 2016 *Nucl. Instr. Meth. A* **816** 176–83

[11] Lamoreaux R H, Hildenbrand D L and Brewer L 1987 *J. Phys. Chem. Ref. Data* **16** 419–43

[12] Allibert M, Chatillon C, Mareschal J and. Lissalde F 1974 *J. Cryst. Growth* **23** 289–94

[13] Bondar I A, Degtyareva V Ya, Tseitlin P A, Derbeneva T A, Mezentseva L P, Raiskaya L N and Domanskii A I 1988 *Russ. J. Inorg. Chem.* **33** 1820–3

[14] Seeley Z M, Cherepy N J and Payne S A 2014 *J. Mater. Res.* **29** 2332–7

[15] Meng F, Koschan M, Melcher C L and Cohen P 2015 *Mat. Sci. Eng. B* **193** 20–6

[16] Kuznetsova D E, Volkov P A, Dosovitskiy G A, Mikhlin A L, Bogatov K B, Retivov V M and

Dosovitskiy A E 2016 *Russ. Chem. Bull., Int. Ed.* in press
[17] Dymov A M and Savostin A P 1958 *Analitical chemistry of gallium* (M: Nauka, in Rus.) p 14